EXPERIMENTS AND MOVIES

Set-up

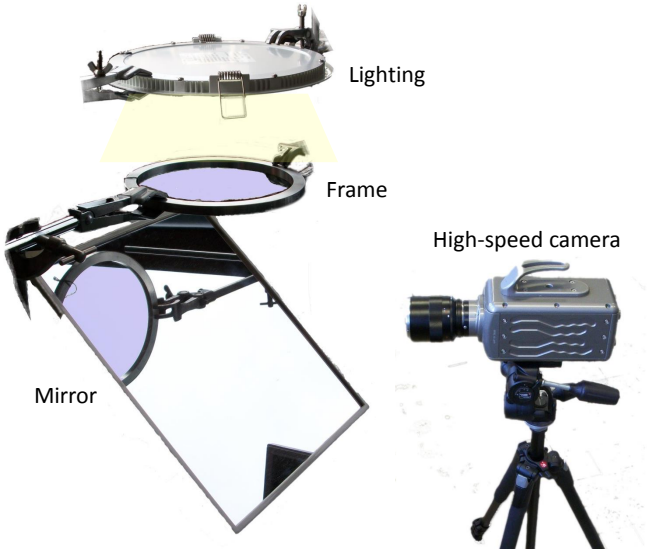

FIG. 1: Experimental set-up allowing us to determine foam film bursting dynamics.

Movies

1. **a.avi** - Movie showing the formation of the aureole during hole expansion. Frame radius is $R = 7$ cm, film thickness is $h_0 = 12$ μm and solution is solution C (see main text). The movie is slowed down 200 times (acquisition frame rate : 6000 Hz).

2. **b.avi** - Movie showing crack-pattern formation during hole opening. Frame radius is $R = 7$ cm, film thickness is $h_0 = 10$ μm and solution is solution E (see main text). The movie is slowed down 450 times (acquisition frame rate : 13500 Hz).

3. **c.avi** -Movie showing irregular hole opening dynamics due to crack pattern. Frame radius is $R = 3$ cm, film thickness is $h_0 = 3$ μm, and solution is solution E (see main text). The movie is slowed down 330 times (acquisition frame rate : 10000 Hz).

NUMERICAL RESOLUTION OF HOLE DYNAMICS IN RADIAL BURSTING

Equations for radial bursting

We describe the radial bursting dynamics of a foam film of initial uniform thickness h_0 and include the effect of dynamic surface tension as first proposed by Frankel and Mysels [1]: the surface tension γ is assumed to depend only on the shrinkage of the surface α which by mass conservation is related to film thickness $\alpha = h_0/h$. We denote the surface elasticity $E(\alpha) = \frac{d\gamma}{d\alpha}$. All the viscous terms are neglected. The capillary forces are then balanced by the fluid inertia of density ρ. All variations of fluid velocity across the film are then neglected and equations are averaged over h. These equations can be explicitly solved in the unidimensional case [1]. However, in the case of radial bursting, a numerical resolution is necessary.

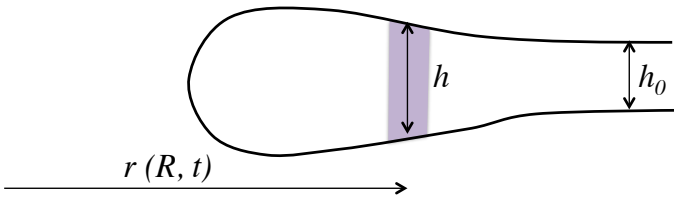

FIG. 2: Profile of the film and notations.

We consider a material element that has initially the position R (*i.e.* that has Lagrangian variables (R,t)). At instant t, its position is $r(R,t)$ and its thickness $h(R,t)$. The fluid velocity is $u = \partial r/\partial t$ and the shrinkage is defined as $\alpha = h/h_0 \partial r^2/\partial R^2 = (r/R)\partial r/\partial R$. The momentum balance on the fluid element yields

$$\rho r h \frac{\partial u}{\partial t} = 2r \frac{\partial \gamma}{\partial r}$$

which can be rewritten

$$\frac{\partial u}{\partial t} = \frac{2E(\alpha)}{\rho h_0} \frac{r}{R} \frac{\partial \alpha}{\partial R} = U_\alpha^2 \frac{r}{R} \frac{\partial \alpha}{\partial R} \tag{1}$$

in which we have defined the characteristic velocity

$$U_\alpha = \sqrt{\frac{2E(\alpha)}{\rho h_0}}.$$

Following the analysis of Frankel and Mysels, we are looking for self-similar solutions in the form $r/t = f(R/t)$. We thus define the variables $W = R^2/(2t^2)$ and $w = r^2/(2t^2)$ (w

and W have the dimensions of square velocities) and we expect $w = w(W)$. The relative shrinkage is also set by $\alpha = dw/dW$. Starting from Eq.1, we find

$$\frac{W}{w}\left[1 - \frac{W}{w}\frac{dw}{dW}\right]\frac{dw}{dW} = \left[U^2_{\alpha=dw/dW} - \frac{2W^2}{w}\right]\frac{d^2w}{dW^2} \tag{2}$$

A first information on the film dynamics can be inferred from this equation: Far from the hole, i.e. for large W, the film should remain undisturbed, which corresponds to $w = W$ and $dw/dW = 1$. This condition combined with Eq.2 yields $\left[U^2_{\alpha=1} - \frac{2W^2}{w}\right]\frac{d^2w}{dW^2} = 0$, which implies that the matching with the disturbed film can only be done at $W = W_0 = U^2_{\alpha=1}/2$. The velocity of the front of the *aureole*, or extended rim corresponding to the disturbed film, is thus given by $u_f = U_{\alpha=1}$ [1].

Finally, the complete aureole profile and hole receding velocity will depend on the form of the elasticity versus shrinkage.

Numerical resolution for a constant elasticity model

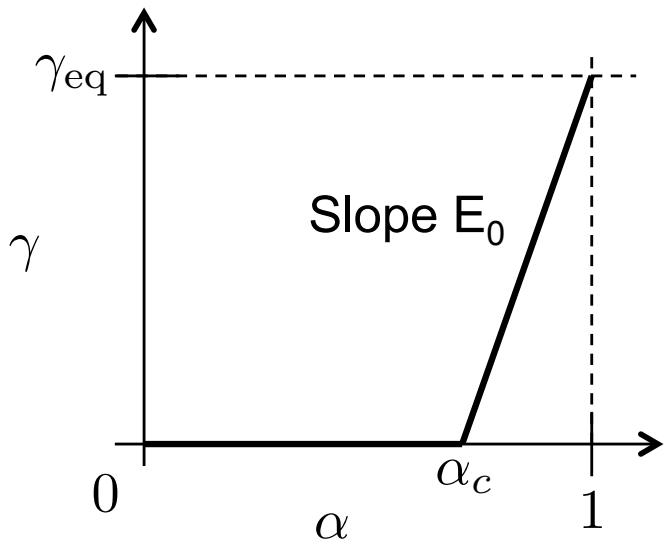

FIG. 3: Variations of surface tension γ versus shrinkage α in the simplified constant elasticity modeling.

We consider at first order a model of constant elasticity E_0, as described in figure 3. We introduce here α_c, which corresponds to the maximum shrinkage the film can endorse. For

$\alpha > \alpha_c$, the surface elasticity is constant and reads

$$\frac{d\gamma}{d\alpha} = E_0 = \gamma_{\text{eq}} \frac{1}{1-\alpha_c}$$

and then

$$U_\alpha = U_0 = \sqrt{\frac{2E_0}{\rho h_0}} = \sqrt{\frac{E_0}{\gamma_{\text{eq}}}}\, V_c$$

where $V_c = \sqrt{2\gamma_{\text{eq}}/(\rho h_0)}$ is Culick velocity.

When $\alpha > \alpha_c$, eq. 2 can be written as

$$\frac{W}{w}\left[1 - \frac{W}{w}\frac{dw}{dW}\right]\frac{dw}{dW} = \left[U_0^2 - \frac{2W^2}{w}\right]\frac{d^2w}{dW^2} \tag{3}$$

In non-dimensionalized form (stating $\tilde{W} = 2W/V_c^2$ and $\tilde{w} = 2w/V_c^2$), this equation reduces to

$$\frac{\tilde{W}}{\tilde{w}}\left[1 - \frac{\tilde{W}}{\tilde{w}}\frac{d\tilde{w}}{d\tilde{W}}\right]\frac{d\tilde{w}}{d\tilde{W}} = \left[\frac{1}{1-\alpha_c} - \frac{2\tilde{W}^2}{\tilde{w}}\right]\frac{d^2\tilde{w}}{d\tilde{W}^2} \tag{4}$$

with the two following boundary conditions:

- In $\tilde{W} = 0$, at the hole, we have the maximum shrinkage (minimum value of α_c): $\frac{d\tilde{w}}{d\tilde{W}}(\tilde{W} = 0) = \alpha_c$.
- In $\tilde{W} = \tilde{W}_0 = \frac{1}{2(1-\alpha_c)}$, at the aureole front, the solution should match the undisturbed film solution $\tilde{w}(\tilde{W}_0) = \tilde{W}_0$.

This equation can then be solved numerically with a shooting method: we start from the initial condition $\tilde{w}(0) = \tilde{w_0}$ and $(d\tilde{w}/d\tilde{W})(0) = \alpha_c$ and find $\tilde{w_0}$ in order to match the condition $\tilde{w}(\tilde{W_0}) = \tilde{W_0}$.

To get to more physical parameters, from the function $w(W)$, we can deduce the thickness profile, using the relation $h/h_0 = 1/(dw/dW)$ (figure 4) for different elasticities. As the elasticity increases (i.e. as α_c becomes closer to 1), we find that the aureole is thinner and wider, while for $E_0 = \gamma_{\text{eq}}$ (corresponding to $\alpha_c = 0$), one recovers a punctual rim receding at Taylor-Culick velocity V_c.

We can also estimate the initial hole velocity $u_0 = \sqrt{2w(W=0)}$, which is shown in figure 5 as a function of the ratio E_0/γ_{eq}. From the comparison between these data and our experimental hole velocities, we can deduce the elasticity of our investigated solutions.

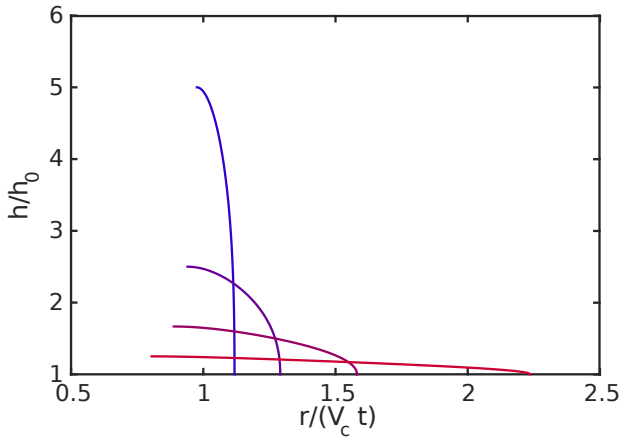

FIG. 4: h/h_0 as a function of $r/(V_c t) = \sqrt{2w/V_c^2}$ for radial bursting and different values of α_C (0.2, 0.4, 0.6, 0.8 from top to bottom at the origin).

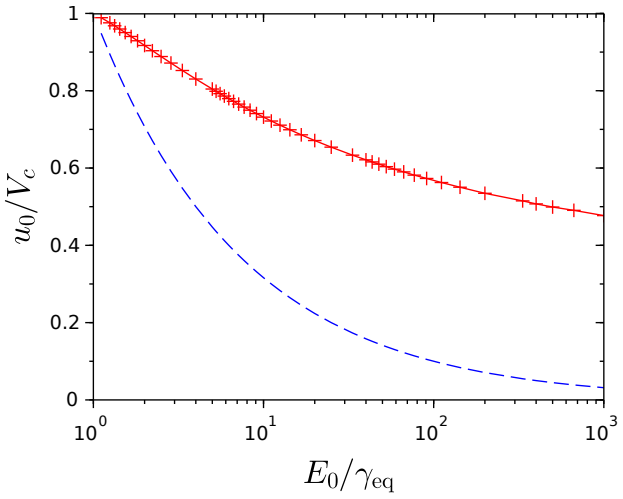

FIG. 5: (+) Normalized hole opening velocity u_0/V_c as a function of $E_0/\gamma_{\rm eq}$ in the model of radial bursting with a constant elasticity. The dashed line corresponds to $u_0/V_c = \sqrt{\gamma_{\rm eq}/E_0}$ expected for unidimensional bursting [1].

We also observe that the results obtained deviate from those obtained for unidimensional bursting [1] , especially for large elasticities, emphasizing the crucial role of radial geometry.

---

[1] S. Frankel and K. J. Mysels, Journal of Physical Chemistry **73**, 3028 (1969).